CHEMISTRY & SUSTAINABILITY

CHEMSUSCHEM

ENERGY & MATERIALS

Accepted Article

Title: Selective Conversion of Cellulose to Hydroxyacetone and 1-Hydroxy-2-Butanone Using Sn-Ni Bimetal Catalysts

Authors: Longlong Ma, Haiyong Wang, Changhui Zhu, Qiying Liu, Jin Tan, Chenguang Wang, and Zheng Liang

To be cited as: *ChemSusChem* 10.1002/cssc.201900172

Link to VoR: http://dx.doi.org/10.1002/cssc.201900172

A Journal of

ChemPubSoc Europe

WILEY-VCH

www.chemsuschem.org

Selective Conversion of Cellulose to Hydroxyacetone and 1-Hydroxy-2-Butanone Using Sn-Ni Bimetal Catalysts

Haiyong Wang[1, 2, 3, 4], Changhui Zhu[1, 2, 3, 4], Qiying Liu[1, 2, 3,5]*, Jin Tan[1, 2, 3], Chenguang Wang[1, 2, 3], Zheng Liang[1,2,3], Longlong Ma[1, 2, 3]*

1 Guangzhou Institute of Energy Conversion, Chinese Academy of Sciences, Guangzhou 510640, P. R. China

2 CAS Key Laboratory of Renewable Energy, Guangzhou 510640, P. R. China

3 Guangdong Key Laboratory of New and Renewable Energy Research and Development, Guangzhou 510640, P. R. China

4 University of Chinese Academy of Sciences, Beijing 100049, P. R. China

5 Dalian National Laboratory for Clean Energy, Dalian 116023, P. R. China

*Author for correspondence: Qiying Liu (liuqy@ms.giec.ac.cn), Longlong Ma (mall@ms.giec.ac.cn)

Hydroxyacetone (HA) and 1-hydroxy-2-butanone (HB), both of which contain carbonyl and hydroxyl groups, are becoming increasingly important as intermediates, due to their diversified applications in fine chemicals production such as medicine and food additives. We developed a strategy to obtain these two products from direct cellulose conversion over Sn-Ni intermetallic compound (IMC) catalysts. It was confirmed that the Sn-Ni IMC and SnO_x acted as the active sites for HA and HB production via selectively cleaving the target C-C and C-O bonds. About 70 % of total HA (33.2%) and HB (35.6%) yield could be obtained by selective hydrogenolysis of cellulose. This strategy expands the application of cellulose for affording a new route to renewably produce the high valued C_3-C_4 keto-alcohols from cellulosic biomass.

With the growing shortage of fossil resources and the increase in greenhouse gas emissions, developing green, rich, renewable carbon sources to replace fossil carbon is the tendency in both the academic and industrial communities.[1,2] Biomass resources are the abundant and sustainable carbon source in nature for the production of high valued platform chemicals.[3,4] Cellulose is the most abundant component in

lignocellulosic biomass. Its linear polysaccharide polymer with numerous hydroxyl groups makes it act as a favorable feedstock for the production of high value-added fine chemicals.[5-14] Fine chemicals, such as pesticides, coatings, drug intermediates, and food additives, used in daily life, are almost petrochemical products.[15] Currently, developing new catalytic strategy to match with the conversion of biomass are increasingly attracted.[16,17]

Most researchers focused on studies for enhancing the activities of hydrogenation and selectively cleaving C-C bond of the catalysts to catalyze the hydrolysis of cellulose. Traditional precious-metal catalysts, such as Ru, Pt, Pd are usually used, and they exhibited relatively high activity. Due to the high activity of the catalysts, the production from cellulose are polyols and C_2-C_6 alcohols.[18-21] For some compounds, the unsaturated C=O bond makes them exhibit special nature and application. Accordingly, a bifunctional catalyst with selectively breaking C-C bond and partial hydrogenation would be a good choice for biomass catalytic conversion. Keto-alcohols, which possess hydroxyl and activity unsaturated carbonyl groups, are among the high value-added organic compounds and could potentially be used for many organics synthesis. In particularly, hydroxyacetone (HA) is an important intermediate used to produce polyols, acrolein, methylglyoxal, acetone and lactic acid or directly used as food addictive, reducing agent and so on.[22-26] The HA produced mainly by oxidation of 1,2-propanediol which is produced mainly from petro-propylene via epoxy compounds.[25,27,28] It also can be obtained by direct conversion cellulose over Ni based catalysts such as Ni-SnO_x/Al_2O_3 or signal-atom Ni catalysts.[27,29,30] In Liu's work, they

investigated the catalytic performances of Ni-SnO_x of with Sn/Ni ratios in a range of 0-2.0, and they proposed that the SnO_x species were responsible for the selective cleavage of the C-C bonds in glucose and fructose.[23] 1-hydroxy-2-butanone (HB) is mainly used to synthesis ethambutol, a most common anti-tuberculosis medicine.[30] It is produced mainly by oxidation of 1,2-butanediol over CuO or enzyme catalyst.[31] The HA and HB are also found in the preparation of polyols by non-selective pyrolysis of biomass, while the both amounts are small with the yields below 10%.[32] For producing HA and HB from direct cellulose hydrogenolysis, developing new catalyst is critical for selectively cleaving the target C-C bond while protecting the target C=O and C-OH bonds survived from partial hydrogenation.

In this work, we for the first time report the synchronized production of HA and HB with a total yield of 70 % through selective cleavage of the C-C bonds by retro-aldol condensation over a Ni_3Sn_4-SnO_x catalyst in water. The bimetallic Sn-Ni IMC was prepared by controlling the Sn/Ni ratio and annealing temperatures. The formation of Ni_3Sn_4 and their synergistic effect with Sn oxide species endow the catalysts unexpected performance in hydrogenolysis of cellulose.

The investigations were started with hydrogenolysis of cellulose on single metal and bimetal Sn-Ni IMC catalysts. The influence of reaction conditions such as reaction time, temperature, and initial H_2 pressure was also investigated (Figure 1, Figure S1 and Table S3). The maximum yield of keto-alcohol was obtained at 240 ^oC, 4 MPa H_2, and with a reaction time of 1 h. Thus, all the catalysts were evaluated under these optimized conditions. Table 1 showed the results of cellulose conversion and the

products distribution over various Sn-Ni catalysts. Catalysis by Ni@C demonstrated a low conversion of cellulose (52.3 %), and the main products were ethylene glycol (EG, 15.3 %) and hexitols (18.3 %). Other products including glucose, sorbitol, 1,2-propanediol (1,2-PDO), glycerol (Gly), lactic acid (La), HA, HB, methylglyoxal (MG) and acetoin (Ace), and the total yield of these products was very low (< 5 %). Only small amount products were detected after the cellulose conversion with Sn@C as the catalyst. The conversion of cellulose was 30 % while the total yield of keto-alcohols was only 5 % (Entry 3, Table 1). Compared to the experiment in which the Ni@C was solely used (Entry 1, Table 1), the products distribution and yields remained almost unchanged over the Ni@C+Sn@C, and EG and hexitol were the main products (Entry 4, Table 1). It is interesting for the 3Sn-Ni@C_T catalysts. When the metal Sn and Ni were introduced into the catalyst simultaneously, the distribution of products significantly changed (Entry 4-9, Table 1). The cellulose conversion has increased to more than 90 %. The yields of HA and HB were obviously increased over the 3Sn-Ni@C_T catalysts. At low annealing temperature, the total yield of HA and HB was 36.2 % (Entry 5, Table 1). As the annealing temperature of catalyst increased, the yield of HA and HB increased. The highest total yield of keto-alcohols was up to 72 % over the 3Sn-Ni@C_{600} catalyst (Entry 8, Table 1). However, with further increasing the annealing temperature, the yields were decreased to 39.3 %. The carbon balance based on total organic carbon (TOC) analysis of the liquid phase showed that there were some amounts of carbon missing. The missing carbon was due to the formation of gas products and the possibly unidentified products (e.g. humins) derived from the

condensation or degradation of glucose and other sugar intermediates. [33]

Table 1. Conversion of cellulose and the products distribution over different NiSn@C catalysts

Catalyst	Conv. (%)	Yield (C-mol%)										Carbon balance (C-mol%)
		EG	1,2-PDO	Gly	La	HA	MG	Ace	HB	T_{k-a}	C_6	
Ni@C	52.3	15.3	3.1	0.2	0	0.3	0.4	0.1	0.4	1.2	18.3	75.1
Ni-NiO@C[a]	67.2	9.1	11.6	0	12.6	0	0	0	0	0	10.1	79.8
Sn@C	30.1	0	0	0	0	3.8	0	0	1.2	5.0	0.8	25.9
Sn@C+Ni@C	62.9	15.6	3.4	0	0	0	0	0	0.2	0.2	20.1	62.8
3Sn-Ni@C_{300}	70.1	4.3	10.4	0.4	3.3	15.3	0.1	2.6	1.1	19.1	7.1	63.4
3Sn-Ni@C_{400}	82.1	0.1	0.1	0.6	0.9	16.1	0.2	1.1	18.6	36.2	5.6	52.7
3Sn-Ni@C_{500}	90.2	0.2	0.4	0.8	1.1	30.4	0.3	2.2	23.7	57.2	4.7	70.7
3Sn-Ni@C_{600}	96.2	0.1	0.6	1.0	1.3	33.2	0.4	2.1	35.6	72.0	0.2	77.4
3Sn-Ni@C_{700}	95.4	2.5	0.6	0.7	0.6	21.8	0.3	1.9	18.9	46.0	0.3	49.3
3Sn-Ni@C_{800}	94.8	3.6	0.7	0.5	0.4	18.9	0.2	1.2	14.7	39.3	0.6	43.0

Reaction conditions: cellulose 0.2 g; catalyst 0.08 g; deionized water 20 mL; reaction temperature 240 °C; reaction time 1 h and initial H_2 pressure 4.0 MPa. T_{k-a} total yield of keto-alcohols; EG, ethylene glycol; 1,2-PDO, 1,2-propanediol; Gly, glycerol; La, lactic acid; HA, hydroxyacetone; MG, methylglyoxal; Ace, acetoin; HB, 1-hydroxy-2-butanone; C_6, sorbitol.

a: main other products, glyceric acid 10.2 %

Screening on *x*Sn-Ni@C_{600} catalysts, the catalytic performances of Sn/Ni catalyst with different atomic ratio are investigated (Figure 1 A). Upon addition of a small amount of Sn to Ni@C at the Sn/Ni ratio of 1.0, the yield of EG and sorbitol decreased rapidly from 33.6 % to 8.8 %, meanwhile, the yields of C_3-C_4 keto-alcohols significantly increased to 41.1 %. When Sn/Ni ratio was increased to 3.0, the sorbitol yield sharply decreased to 0.5 % with the concurrent increase of the C_3-C_4 keto-alcohols to 72 % for obtaining the main respective products of HA (33.2 %) and HB (35.6 %). However, further increasing the Sn/Ni ratios to 4.0 and 5.0 led to an obvious decrease in the C_3-C_4 keto-alcohols yields to 46.3% and 16.1 %, respectively. The catalytic

behavior of the 3Sn-Ni@C_{600} catalyst is shown in Figure 1B, HA and HB were formed at yields of 19.7% and 21.1% in 30 min, respectively. As the precursor of HA, glyceraldehyde was detected during the reaction with the yield of 5.1% and then disappeared at 1 h. The HA and HB were produced at yields of 33.2% and 35.6% in 1 1, respectively. Further prolonging the reaction time, the yield of keto-alcohols decreased slightly.

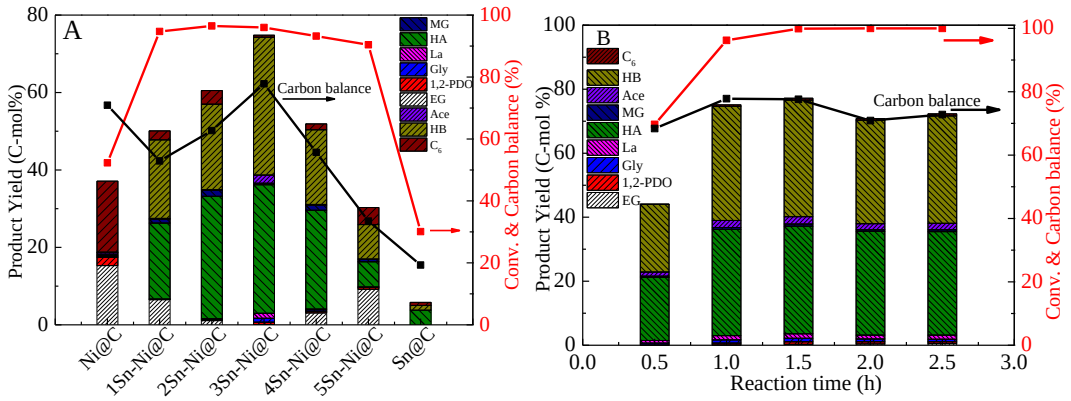

Figure 1. Effect of Sn/Ni atomic ratios (A) and reaction time over 3Sn-Ni@C_{600} (B) on cellulose conversion and products yield.

Reaction conditions: cellulose 0.2 g; catalyst 0.08 g; deionized water 20 mL; reaction temperature 240 °C; reaction time (A) 1 h, (B) 0.5-2.5 h, and initial H_2 pressure 4.0 MPa. EG, ethylene glycol; 1,2-PDO, 1,2-propanediol; Gly, glycerol; La, lactic acid; HA, hydroxyacetone; MG, methylglyoxal; Ace, acetoin; HB, 1-hydroxy-2-butanone; C_6, sorbitol, glucose.

Figure 2A showed the XRD patterns of monometallic and bimetallic Sn-Ni catalysts. Clearly, the monometallic Ni@C sample exhibited the characteristic (111) and (200) diffractions of crystalline metallic nickel (JCPDS 04-0850). With Sn introduced (Sn/Ni ratio of 1.0 and 2.0), some new peaks which attributed to Sn-Ni IMC (Ni_3Sn_2 and Ni_3Sn_4) and SnO_x could be observed. The dominant Sn-Ni phase in these

two catalysts was Ni_3Sn_2. In addition, the absence of metal Ni also reflected the formation of bimetallic Sn-Ni IMC phases. At the Sn/Ni atomic ratio of 3.0 and 4.0, the Sn-Ni IMC existed primarily in the form of Ni_3Sn_4. Further increasing the Sn/Ni ratio to 5.0, the diffractions of Sn-Ni IMC disappeared, and diffractions of Sn oxide species were observed. While for the Sn@C catalyst, the Sn species existed primarily in the form of SnO_x and metallic Sn. The annealing temperature also affected the component of the Sn-Ni catalysts. Sn-Ni IMC catalysts were prepared via reduction-carbonation of the precursor at different annealing temperatures in a nitrogen atmosphere. During the carbonation process, CH_4, CO and C from the precursor reduced the Sn^{2+} and Ni^{2+} to metal Sn and Ni (Figure S2). Subsequently, the Sn-Ni IMC formed with the temperature increased. As shown in Figure S3, the main peaks of 3Sn-Ni@C_{300} were SnO_x and Ni_3Sn_2. With the annealing temperature increased from 300 to 600 ^oC, the peaks of SnO_x and Ni_3Sn_2 decreased and the intensity of the characteristic diffraction peaks corresponding to Ni_3Sn_4 increased. The BET surface of the catalysts was also increased from 2.1 to 403.5 m^2/g with the annealing temperature increased from 300 ^oC to 600 ^oC. Correspondingly, the keto-alcohol yields increased from 19.1 % to 72.0 %. These results (Entry 5, Table 1) showed that the Ni_3Sn_4, rather than the Ni_3Sn_2, is the active phase for the formation of HA and HB. However, further increasing the annealing temperature led to a significant loss in keto-alcohols yield. The decrease of Ni_3Sn_4 content (Figure S3 and Table S1) may be responsible for the reduction of the keto-alcohols.

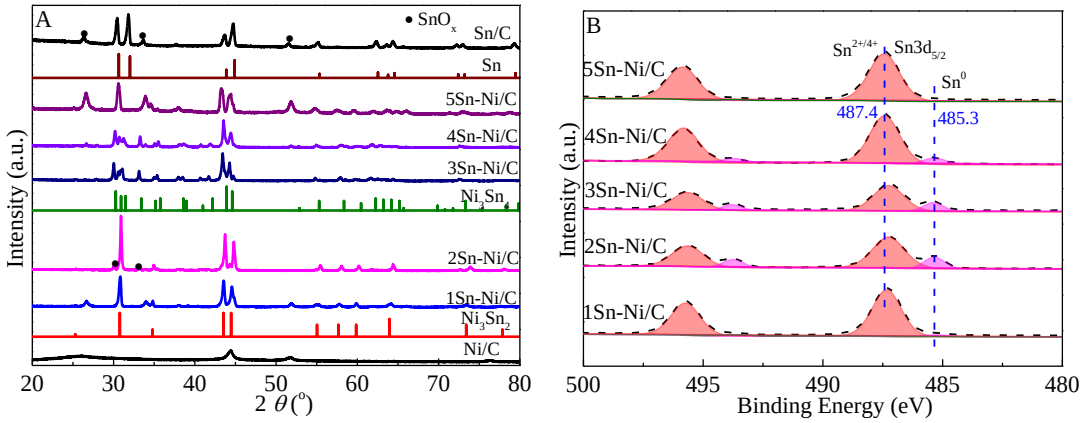

Figure 2. XRD patterns (A) and Sn 3d (B) of *x*Sn-Ni@C catalysts annealed at 600 °C.

The surface chemical states of the catalysts were studied by XPS analysis. As shown in Figure 2B, two groups of peaks were detected on the surface of *x*Sn-Ni@C_{600} catalysts. The higher binding energy at 487.4 eV (Sn $3d_{5/2}$) and 495.9 eV (Sn $3d_{3/2}$) were assigned to the oxidized Sn species (Sn^{2+} and Sn^{4+}), but the distinction between Sn^{2+} and Sn^{4+} was difficult owing to the negligible difference in the binding energies.[34] The other group of peaks with binding energy at 485.3 eV (Sn $3d_{5/2}$) and 493.8 eV (Sn $3d_{3/2}$) were attributed to the metallic Sn species (Sn^0). The XPS results indicated that, the Sn species on the Sn-Ni catalysts surface mainly existed in the form of SnO_x, and a not negligible part (2-20 %) Sn existed in the form of Sn-Ni IMC (Table S1). The Ni $2p_{3/2}$ region comprises the main peak, the shoulder, and its satellites at 853.0, 856.2 and 862.0 eV, respectively (Figure S4). The peak around 856 eV is attributed to $Ni^{\sigma+}$, which could act as Lewis acid site in the reaction (Figure S5 and Table S4).[35,36]

For *x*Sn-Ni@C_{600} catalysts ($2.0 < x < 5.0$), the Sn/Ni mole ratio was higher than the nominal ones at 4:3 or 2:3 of Sn-Ni IMCs. Therefore, it could be speculated that not all Sn formed the Sn-Ni IMC with Ni. In other words, some Sn-Ni intermetallic particles might be formed non-uniformly or some SnO_x might exist on the 3Sn-

$Ni@C_{600}$.[37] This result was consistent with the TEM images (Figure 3 and Figure S7). The Ni_3Sn_4 IMC and SnO_x particles with the average size 25.4 nm were clearly found to be well dispersed in the carbon matrix. The lattice distances of 0.293 nm could be attributed to the (111) plane of Ni_3Sn_4, which was in good agreement with the XRD result.[27,38] SnO_x particles were also observed, and the lattice distance of 0.334 nm was attributed to the (110) plane of SnO_2. The image of Figure 3B further shows that crystalline Sn-Ni IMC was directly attached on SnO_2 particles for forming the distinct boundaries.

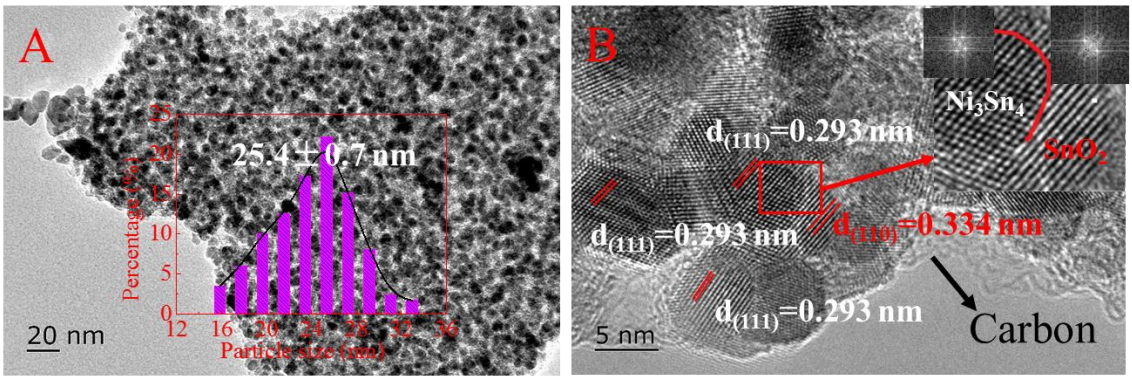

Figure 3. HRTEM images of 3Sn-Ni@C_{600} catalyst.

Table 2. Cellulose conversion and product distribution using different substrates over *x*Sn-Ni@C_{600}

Catalyst	Substrate	Conv. (%)	Yield (C-mol%)									Carbon balance (C-mol%)
			EG	Gly	La	1,2-PDO	HA	MG	Ace	HB	Sor	
3Sn-Ni@C_{600}	sorbitol	0	0	0	0	0	0	0	0	0	100	-
3Sn-Ni@C_{600}	glucose	96.7	0.1	3.3	2.6	0.1	35.2	0.1	0.1	36.1	7.6	88.1
3Sn-Ni@C_{600}[a]	glucose	86.4	0.1	0.9	0.6	0.2	28.1	0	0	30.2	9.7	80.1
Sn@C[a]	glucose	65.4	0.2	0.2	0.1	0.1	2.6	0.1	0.4	1.5	2.7	30.1
3Sn-Ni@C_{600}	fructose	97.9	0.1	1.4	0.9	0.1	46.6	0.1	0.1	2.4	5.3	58.2
3Sn-Ni@C_{600}	erythritol	0	0	0	0	0	0	0	0	0	-	-
3Sn-Ni@C_{600}	glyceraldehyde	95.4	0	10.6	3.4	1.2	74.4	3.4	0	0	-	97.5
3Sn-Ni@C_{600}	glycerol	0	0	100	0	0	0	0	0	0	-	-
Ni@C	sorbitol	0	0	0	0	0	0	0	0	0	100	-
Ni@C	glucose	100	1.2	8.4	18.9	10.3	0	0	0	0	18.6	70.9
Ni@C	fructose	100	0.1	20.6	0	8.7	0	0	0	0	26.4	55.8
Ni@C	erythritol	0	0	0	0	0	0	0	0	0	0	-

Ni@C	glyceraldehyde	100	0	12.9	8.1	76.6	0	0	0	0	0	97.6
Ni@C	glycerol	0	0	100	0	0	0	0	0	0	0	-

Reaction conditions: substrate 0.2 g, catalyst 0.08 g, deionized water 20 mL, reaction temperature 240 °C, reaction time 1 h and initial H_2 pressure 4.0 MPa. EG, ethylene glycol; Gly, glycerol; La, lactic acid; 1,2-PDO, 1,2-propanediol; HA, hydroxyacetone; MG, methylglyoxal; Ace, acetoin; HB, 1-hydroxy-2-butanone; Sor, sorbitol.

a: reaction time 10 min; including other products: fructose (8.9%), ethanol (1.3%), 1,2-butanediol (0.7%), 2,3- butanediol (0.9%), and several unknown products.

In order to understand the reaction pathway for the conversion of cellulose to keto-alcohols, reactions of the possible intermediates, such as sorbitol, glucose, fructose, and other possible intermediates were performed using different catalysts under the comparable reaction conditions to cellulose. Sorbitol was found to be inactive with a negligible conversion after 1 h (Entry 1, Table 2) over the 3Sn-Ni@C_{600} catalyst. In the presence of Sn-Ni intermetallic phase, glucose was converted to the keto-alcohols for obtaining the total yield of 71.5 % (at 96.7 % conversion, Entry 2, Table 2), which showed the similar product distribution to those obtained in cellulose reaction (Entry 8, Table 1). The main products are HA (35.2 %), and HB (36.1 %). While using fructose as a substrate, HA was formed dominantly in the yield of 46.6 % while trace amount of HB (2.4 %) was obtained. These results indicated that HA was produced mainly by direct retro-aldol reaction of fructose over these Sn-Ni catalysts. The reaction results of erythritol and glycerol, the possible intermediates, suggested that they were inactive (Entry 6 and 8, Table 2) for HA and HB production. For glyceraldehyde, the main product was HA (74.4 %, Entry 7, Table 2). However, when using Sn@C physically

mixed with Ni@C as the catalyst, the keto-alcohols were negligible (Table 1). The results showed that Sn-Ni IMC catalyzed the hydrodeoxygenation of C-O in intermediate and also has weak C-C bond cleavage capability for the formation of the keto-alcohols. Therefore, glucose and fructose produced from glucose isomerization are the key two intermediates for highly selective production of HA and HB, respectively, through retro-aldol condensation followed by selective cleavage the C-O bonds over the catalysts (Figure S11).

To identify the functions of different active sites such as SnO_x, Ni metal, NiO and Sn-Ni IMC on the catalysts. A series reactions using cellulose, sorbitol, glucose, fructose, and other possible intermediates as the feedstock were performed over the catalysts including Ni@C, Ni-NiO@C, NiO, Sn@C. The results are listed in Table 1, Table 2 and Table S2. In the presence of Ni@C, despite glucose was completely converted at 1 h, giving La and sorbitol as main products together with the minor C_2-C_3 diols (Entry 10, Table 2) [39]. The C_3-C_4 keto-alcohols was negligible in this case. For the Sn@C catalyst (Entry 4, Table 2), about 65 % of glucose was converted after 10 min of reaction. HA, HB and fructose were observed with yields of 2.6 %. 1.5% and 8.9 %, respectively. Correlating to the characterization results of Sn@C catalyst discussed above (XRD, Figure 2A), the Sn metal and SnO_x on the catalyst provide the major active sites for the glucose isomerization and the retro-aldol condensation of glucose in view of the C_3-C_4 keto-alcohols formation [27,40,41]. For Ni-NiO@C and Sn@C catalysts, the unreduced Ni species and SnO_x act as acid sites and catalyze the degradation of cellulose (Entry 1, Table S2 and Entry 4, Table 2)[42]. Furthermore, NiO

could also inhibit the C-O bond cleavage over Ni particle (Entry 10,11 and 13, Table 2, and Table S2). Based on the results of reaction and characterizations on Sn-Ni catalysts, it is clear that there is a synergetic effect between Sn-Ni IMC and Sn/Ni oxides in the reactions involving cellulose degradation. SnO_x and unreduced Ni catalyzed the glucose isomerization to fructose. The unreacted glucose and produced fructose were further degraded via the retro-aldol condensation on the sites of Sn-Ni IMC and metal oxide on the catalysts. Finally, the C_3 and C_4 intermediates of glyceraldehyde, 1,3-dihydroxyacetone and erythrose were hydrodeoxygenated over Sn-Ni IMC sites to produce C_3-C_4 keto-alcohol.

Considered the results discussed above, it suggested that the formation of the C_3 (HA) and C_4 (HB) products in the cellulose reaction involved the isomerization of glucose to fructose prior to its retro-aldol condensation on the SnO_x species, which was consistent with the observed conversion of glucose to fructose, as shown in Table 2, on the Sn@C and 3Sn-Ni@C_{600} at 240 ºC with 10 min reaction. Davis *et al.*[41] found that Sn incorporated in the framework of zeolite Beta, performed the isomerization reaction following an intramolecular hydride shift mechanism between the carbonyl containing C-1 and hydroxyl bearing C-2 of glucose by a way of a five member complex. Therefore, a similar mechanism of SnO_x is proposed in Scheme 1 and Scheme 2, considering the isomerization on Lewis acid sites (Figure S5 and Table S3) provided by SnO_x. As it is widely known that more vacant orbitals in *d* band would lead to a stronger ability of adsorbing and bonding. With *d* band holes, it can form adsorption bonds with reaction molecules to produce a reactive intermediate[43]. Therefore, the less vacant *d* bands, the

10.1002/cssc.201900172

weaker the hydrogenation capacity of the metal. Ni[$3d^{9.4}4s^{0.6}$] has 0.6 holes, while *d* band in Sn[$4d^{10}5s^{2}5p^{2}$] is full[43,44]. For Sn-Ni IMC, electrons in *d* band of Sn can be occupied the holes of *d* band in Ni metal, and then weaken the hydrogenation capacity of Ni metal. Therefore, the C=O group can be maintained over Sn-Ni IMC with inferior hydrogenation capacity.

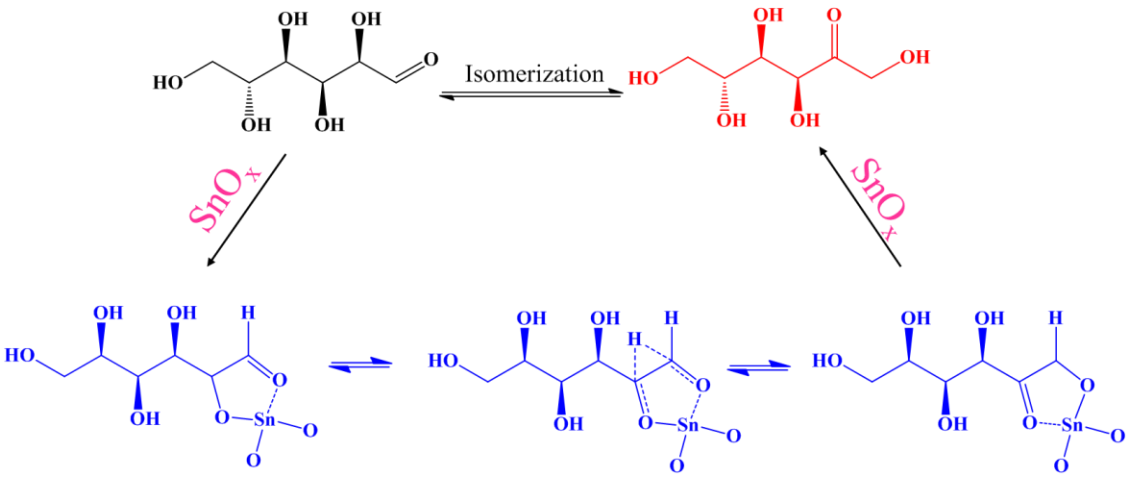

Scheme 1. Isomerization mechanism of glucose to fructose on 3Sn-Ni@C_{600}.

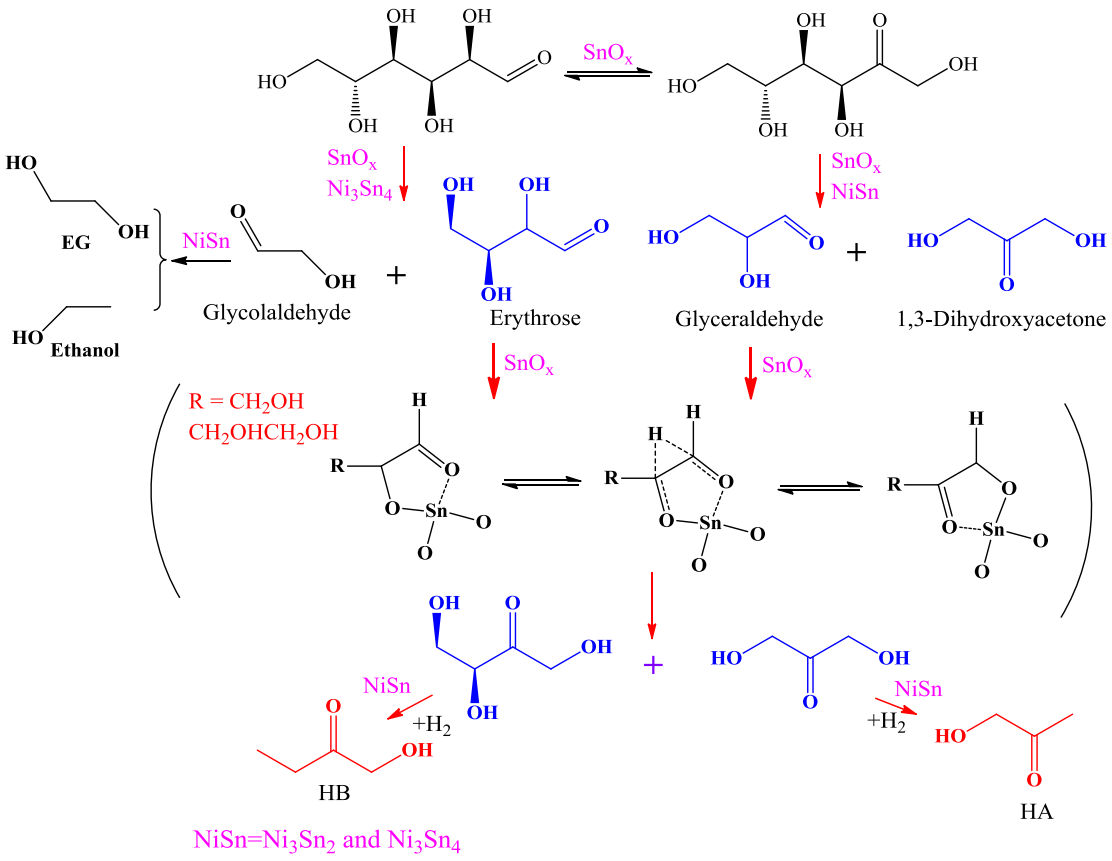

Scheme 2. Reaction scheme for conversion sugars to C_3-C_4 keto-alcohols over 3Sn-Ni@C_{600}.

The recyclability of these Ni promoted catalysts was also examined. As shown in Figure S8. The results showed that the 3Sn-Ni@C_{600} catalyst exhibited good reusability, as indicated by only slight losses in cellulose conversion and keto-alcohols yield. ICP analysis of the reaction solution suggested that leaching of either Ni or Sn is negligible (Entry 7, Table S1). In addition, the good stability of the Sn-Ni IMC could be attributed to the strong interactions between the Ni and Sn species. A slight losses in cellulose conversion and keto-alcohols yield were observed after six cycles either on 3Sn-Ni@C_{600} (representative results in Figure S8). The characterizations of pristine and spent catalysts were also studied (Figure S9). After 6 runs, the particle size of the Sn-Ni intermetallic increased. Considering the residue of cellulose (Figure S9C), the TG-DTA suggested that no obvious carbon deposits on the catalyst (Figure S9D and E).

These results demonstrate that the Sn-Ni catalysts were stable and reusable under the reaction conditions in this work.

In conclusion, we have found that Sn-Ni IMC-SnO_x catalysts (*x*Sn-Ni@C_T) are efficient in the acceleration of the hydrolysis of cellulose to keto-alcohols especially HA (33.2 %) and HB (35.6 %) in water. The Sn-Ni IMC and SnO_x synergistic catalyze cellulose into HA and HB in an aqueous phase. Both the SnO_x and Sn-Ni IMC sites are active sites for cellulose conversion to keto-alcohols. The formation of keto-alcohols are strongly depend on the synergy of Sn-Ni IMC and SnO_x active sites on the surface of the catalysts. Sn-Ni IMC catalyzes the hydrodeoxygenation of C-O in intermediates and has weak C-C bond cleavage capability. The SnO_x can promote the reactions involving cellulose degradation, intermediates isomerization. Glucose and fructose are the key intermediate for highly production of HB and HA, respectively. The *x*Sn-Ni@C catalysts reveal to be an efficient, reusable, and cheap catalyst make of abundant biomass for the fine chemicals in water, and the process environmentally benign and sustainable.

Acknowledgement

This work is financially supported by the National Natural Science Foundation of China (51576199, 51536009), the DNL Cooperation Fund, CAS (DNL180302), the Natural Science Foundation of Guangdong Province (2017A030308010) and the Local Innovative and Research Teams Project of Guangdong Pearl River Talents Program (2017BT01N092).

Reference

[1] D. M. Alonso, J. Q. Bond, J. A. Dumesic, *Green Chem* 2010, **12**, 1493-1513.
[2] M. J. Climent, A. Corma, S. Iborra, *Cheminform* 2014, **16**, 516-547.
[3] J. Carlos Serrano-Ruiz, R. Luque, A. Sepulveda-Escribano, *Chem. Soc. Rev.* 2011, **40**, 5266-5281.
[4] C. Li, M. Zheng, A. Wang, T. Zhang, *Energ. Environ. Sci.* 2012, **5**, 6383-6390.
[5] J. Pang, M. Zheng, R. Sun, L. Song, A. Wang, X. Wang, T. Zhang, *Bioresour Technol* 2015, **175**, 424-429.
[6] H. Tang, N. Li, F. Chen, G. Li, A. Wang, Y. Cong, X. Wang, T. Zhang, *Green Chem* 2017, **19**, 176-182.
[7] G. W. Huber, S. Iborra, A. Corma, *Chem. Rev.* ***2006***, *106*, 4044-4098.
[8] P. A. Lazaridis, S. A.Karakoulia, C. Teodorescu, N. Apostol, D. Macovei, A. Panteli, A. Delimitis, S. M. Coman, V. I. Parvulescu, K. S. Triantafyllidis, *Appl Catal B-Environ* 2017, **214**, 1-14.
[9] J. Xi, Q. Xia, Y. Shao, D. Ding, P. Yang, X. Liu, G. Lu, Y. Wang, *Appl Catal B-Environ* 2016, **181**, 699-706.
[10] J. Keskivali, S. Rautiainen, M. Heikkila, T. T. T. Myllymaki, J.-P. Karjalainen, K. Lagerblom, M. Kemell, M. Vehkamaki, K. Meinander, T. Repo, *Green Chem* 2017, **19**, 4563-4570.
[11] B. Zhang, X. Li, Q. Wu, C. Zhang, Y. Yu, M. Lan, X. Wei, Z. Ying, T. Liu, G. Liang, F. Zhao, *Green Chem* 2016, **18**, 3315-3323.
[12] N. Ji, T. Zhang, M. Y. Zheng, A. Q. Wang, H. Wang, X. D. Wang, J. G. G. Chen, *Angew Chem Int Edit* 2008, **47**, 8510-8513.
[13] L. Gao, Y. Bao, S. Gan, Z. Sun, Z. Song, D. Han, F. Li, L. Niu, *ChemSusChem* 2018, 10.1002/cssc.201800695.
[14] M. Ventura, D. Williamson, F. Lobefaro, M. D. Jones, D. Mattia, F. Nocito, M. Aresta, A. Dibenedetto, *ChemSusChem* 2018, **11**, 1073-1081.
[15] M. Ventura, F. Nocito, E. D. Giglio,S. Cometa, A. Altomare, A. Dibenedetto, *Green Chem* 2018, **20**, 3921-3926.
[16] L. I. I. Granone, F. Sieland, N. Zheng, R. Dillert, D. W. Bahnemann, *Green Chem* 2018, **20**, 1169-1192.
[17] H. Kobayashi, T. Komanoya, S. K. Guha, K. Hara, A. Fukuoka, *Appl Catal A Gen* 2011, **409**, 13-20.
[18] J. Yi, S. Liu, M. M. Abu-Omar, *ChemSusChem* 2012, **5**, 1401-1404.
[19] C. Luo, S. Wang, H. Liu, *Angew Chem Int Edit* 2010, **119**, 7780-7783.
[20] J. Sun, H. Liu, *Chinese J Catal* 2011, **13**, 135-142.
[21] B. Gumina, F. Mauriello, R. Pietropaolo, S. Galvagno, C. Espro, *Mol Catal* 2018, **446**, 152-160.
[22] S. Sato, D. Sakai, F. Sato, Y. Yamada, *Chem Let* 2012, **41**, 965-966.
[23] T. Deng, H. Liu, *J Mol Catal A-Chem* 2014, **388**, 66-73.
[24] Y. Wang, M. Zhuang, S. Chen, W. Hu, J. Sun, J. Lin, S. Wan, Y. Wang, *ACS Catal* 2017, **7**, 6038-6047.
[25] A. K. Kinage, P. P. Upare, P. Kasinathan, Y. K. Hwang, J.S.Chang, *CatalCommun* 2010, **11**, 620-623.
[26] V. Zacharopoulou, E. S. Vasiliadou, A. A. Lemonidou, ChemSusChem 2018, **11**, 264-275.

[27] R. Sun, M. Zheng, J. Pang, X. Liu, J. Wang, X. Pan, A. Wang, X. Wang, T. Zhang, *ACS Catal* 2016, **6**, 191-201.
[28] M. Zheng, J. Pang, R. Sun, A. Wang, T. Zhang, *ACS Catal* 2017, **7**, 1939-1954.
[29] W. Liu, Y. Chen, H. Qi, L. Zhang, W. Yan, X. Liu, X. Yang, S. Miao, W. Wang, C. Liu, A. Wang, J. Li, T. Zhang, *Angew Chem Int Edit* 2018, **57**, 7071-7075.
[30] C. W. Chin, M. A. Dasari, G. J. Suppes, W. R. Sutterlin, *AIChE J* 2006, **52**, 3543-3548.
[31] L. G. Lee, G. M. Whitesides, *J Org Chem*1986, **51**, 25-36.
[32] A. Demirbas, *Fuel Process Technol* 2007, **88**, 591-597.
[33] H. Wang, C. Zhang, Q. Liu, C. Zhu, L. Chen, C. Wang, L. Ma, *ACS Energ Fuel* 2018, **32**, 11529-11537.
[34] J. M. Jacob, P. G. Corradini, E. Antolini, N. A. Santos, J. Perez, *Appl Catal B-Environ* 2015, **165**, 176-184.
[35] X. Yan, J. Zheng, L. L. Zheng, G. Lin, H. Lin, G. Chen, B. Du, F. Zhang, *Mater Res Bull* 2018, **103**, 150-157.
[36] J. W. Shabaker, D. A. Simonetti, R. D. Cortright, J. A. Dumesic, *J Catal* 2005, **231**, 67-76.
[37] J. Liu, Y. Wen, P. A. van Aken, J. Maier, Y. Yu, *NANO Let* 2014, **14**, 6387-6392.
[38] J. W. Jang, P. G. Kim, K. N. Tu, D. R. Frear, P. Thompson, *J Appl Phys* 1999, **85**, 8456-8463.
[39] M. F. N. D'Angelo, V. Ordomsky, J. van der Schaaf, J. C. Schouten, T. A. Nijhuis, *ChemSusChem* 2014, **7**, 627-630.
[40] J. Pang, M. Zheng, X. Li, Y. Jiang, Y. Zhao, A. Wang, J. Wang, X. Wang, T. Zhang, *Appl Catal B-Environ* 2018, **239**, 300-308.
[41] R Y. Roman-Leshkov, M. Moliner, J. A. Labinger, M. E. Davis, *Angew Chem Int Edit* 2010, **49**, 8954-8957.
[42] S.Van de Vyver, J. Geboers, W. Schutyser, M. Dusselier, P. Eloy, E. Dornez, J. W. Seo, C. M. Courtin, E. M. Gaigneaux, P. A. Jacobs, B. F. Sels, *ChemSusChem* 2012, **5**, 1549-1558.
[43] X. Shi, H. Huang, B. Jacobson, Y.-C. Chang, Q.-Z. Yin, C. Y. Ng, *Astrophys J* 2012, **747**, 1-8.
[44] A. Onda, T. Komatsu, T. Yashima, *Phys Chem Cheml Phys* 2000, **2**, 2999-3005.